EARTHQUAKE-INDUCED EARTH PRESSURES ON RETAINING WALLS

by R. F. Scott[I]

SYNOPSIS

A model for the dynamic behaviour of a soil-retaining wall system is presented. From the model, expressions are derived for the pressures, forces, and moments which may act on the wall during a design earthquake. In the analysis, modifications enable the variation of soil properties with depth and the flexibility of the wall to be taken into account.

INTRODUCTION

The calculation of the pressures developed on retaining structures by earthquake vibration is generally based on a static Coulomb wedge analysis with the addition of a horizontal acceleration, as suggested by Mononobe (4) and Okabe (5). Such an analysis leads to a pressure distribution on the wall increasing linearly from top to bottom. An evaluation of the Mononobe-Okabe calculation method has been given by Seed and Whitman (6). They conclude from small-scale experiments of the investigators that the calculated force on the wall is approximately correct. However they point out that to give the measured base moment, the calculated force must be applied at a height of about 0.6 of the wall height from the base, rather than 0.33. There are a number of disadvantages with this theory. It does not represent the dynamic conditions which occur, particularly with respect to large walls, during an earthquake. The relation of a static seismic coefficient to a given design earthquake is tenuous. No accounting for the flexibility of the wall is possible in the analysis. In this paper, an alternative design method will be described. It conforms more closely to the approaches currently in use in structural analysis.

DYNAMIC ANALYSIS

In Fig.1 is shown a two-dimensional cross section through a typical wall and backfill with horizontal surface. It is supposed that the design earthquake input is known at the level AB of the problem profile and that the region of soil ABCD constitutes the backfill or natural soil and backfill adjacent to the wall. In the analysis to be discussed here the soil is treated as a one-dimensional shear beam attached to the wall or walls by springs representing the soil-wall interaction. In the shear-beam method of calculating the dynamic pressure on the retaining wall, either a lumped parameter (Fig.2), or a continuous shear beam (Fig.3) may be employed.

I Professor of Civil Engineering, California Institute of Technology, Pasadena, California, 91109, U.S.A.

CONTINUOUS SHEAR BEAM

The geometry, variables, and properties are shown in Fig.3. In this arrangement the shear beam is connected to the wall BC and the left-hand boundary AD by a continuous Winkler spring foundation of spring constant k. For this model, a resisting pressure is developed at each level, x, of the shear beam proportional to the instantaneous lateral displacement u at that level. In general, the soil properties of density, ρ, Young's modulus, E, and shear modulus, G will vary with depth so that the density and shearing stiffness of the beam, as well as the spring constant k, will also vary with depth. For generality, also, the wall should be considered flexible, but this case will be deferred until later in the paper. The wall is considered to be rigid at first. Various cases of property variation with depth will be considered in order. Damping is left for later inclusion with the selected spectra of ground motion.

(a) Properties constant with depth

In this case the equation of motion is

$$\frac{\partial^2 u}{\partial t^2} = \frac{G}{\rho}\frac{\partial^2 u}{\partial x^2} - \frac{2ku}{\rho b} \tag{1}$$

Solving in the usual way by separation of the time and space variables shows the deflected shape of the beam to be a cosine function, harmonic in time, t, with frequency ω,

$$u = D \cos \lambda x \sin \omega t, \tag{2}$$

where D is a constant for each mode and the various modes of vibration are given by the requirement that

$$D \cos \lambda h = 0 \tag{3}$$

where h is the wall height.

Thus, for the successive mode shapes, λ has the values

$$\lambda_1 = \pi/2h;\ \lambda_2 = 3\pi/2h;\ \cdots\cdots\cdots\ \lambda_n = (2n-1)\pi/2h \tag{4}$$

Substitution of Eq.(2) in Eq.(1) gives the frequencies of the modes

$$\omega_n = \left[\frac{(2n-1)^2\pi^2 G}{4h^2\rho} + \frac{2k}{b\rho}\right]^{1/2} \tag{5}$$

The first term on the right-hand side of Eq.(5) is the frequency of the unrestrained one-dimensional shear beam; the effect of the restraining springs is indicated in the second term.

The participation factors α_n are given by the equation

$$\alpha_n = \frac{\int_o^h \rho(x) X_n(x)\,dx}{\int_o^h \rho(x) X_n^2(x)\,dx} \tag{6}$$

where $X_n(x)$ is the deflected shape of the shear beam in the nth mode. Here, with constant density,

$$\alpha_n = \frac{\int_o^h \cos\lambda_n x\ dx}{\int_o^h \cos^2\lambda_n x\ dx} = \frac{4\sin\lambda_n h}{2\lambda_n h + \sin 2\lambda_n h} \tag{7}$$

The maximum deflection, u_{mn}, associated with a particular mode, at the elevation x, due to a specified design earthquake is given by the equation

$$u_{mn} = \frac{S_{vn}\alpha_n \cos(\lambda_n x)}{\omega_n} \tag{8}$$

where S_{vn} is the relative velocity response at the frequency ω_n in the spectrum used for design purposes, with suitable damping.

The "most probable" deflection at elevation x, u_{mp}, is found from a root-mean-square summation

$$u_{mp} = \left\{\sum_1^\infty \left[\frac{S_{vn}\alpha_n \cos(\lambda_n x)}{\omega_n}\right]^2\right\}^{1/2} \tag{9}$$

The most probable pressure at this elevation p_{mp} is given by the expression

$$p_{mp} = k u_{mp} \tag{10}$$

From the most probable pressure distribution values of a most probable total force and moment can be calculated.

Analysis, by this method, of problems with typical dimensions and soil properties shows that the first mode is principally responsible for the pressure distribution on the wall during the design earthquake; the higher modes contribute substantially smaller pressures. Under these conditions, the equations for the most probable displacement and pressure distribution can be considerably simplified, since only the first mode need be taken into account.

$$\omega_1 = \left(\frac{\pi^2 G}{4h^2\rho} + \frac{2k}{b\rho}\right)^{1/2} \tag{11}$$

$$\lambda_1 = \pi/2h \tag{12}$$

$$\alpha_1 = \frac{4}{\pi} \tag{13}$$

and the first mode shape is

$$u_1 = D\cos\frac{\pi x}{2h} \tag{14}$$

Consequently the maximum deflection u_{m_1} (equal in the absence of other modes, to the most probable deflection) is given from Eqs.(8), (11), (12) and (13) to be

$$u_{m_1} = \frac{4S_{v1}}{\pi\omega_1}\cos\left(\frac{\pi x}{2h}\right) \tag{15}$$

From Eqs.(10) and (15) the maximum pressure distribution p_{m_1} on the wall is also a cosine function

$$p_{m_1} = \frac{4kS_{v1}}{\pi\omega_1}\cos\left(\frac{\pi x}{2h}\right) = p_o\cos\left(\frac{\pi x}{2h}\right) \tag{16}$$

in which p_o, the maximum pressure at ground surface, is given by the equation

$$p_o = \frac{4kS_{v1}}{\pi\omega_1} \tag{17}$$

The total maximum force on the wall P_{m_1} per lineal foot is given by the area under the cosine pressure distribution curve

$$P_{m_1} = \frac{2}{\pi}p_o h \tag{18}$$

The point of action of this force is located $2h/\pi$ above the base of the wall, as compared with h/3 in the Mononobe-Okabe method. The location of the maximum force compares with the empirically-modified Mononobe-Okabe value of 0.6h as suggested by Seed and Whitman (6).

The maximum moment at the base M_{m_1} per lineal foot is

$$M_{m_1} = \frac{2P_{m1}h}{\pi} = \frac{4}{\pi^2}p_o h^2 \tag{19}$$

It would be of interest at this stage to obtain a calibration as to the accuracy with which the shear beam-Winkler model yields the natural frequency of at least the first mode. A two-dimensional solution has been obtained by Wood (7) to the problem of Fig.1 when no vertical displacements are permitted. This artificial restraint will cause the resulting frequencies to be too high in comparison with a solution in which both displacements occur. A comparison between Wood's solution for the first mode and Eq.(11) indicates that the two frequencies will be close if b = L and

$$k = \frac{4E(1-\nu)}{L(1+\nu)(1-2\nu)} = \frac{8G(1-\nu)}{L(1-2\nu)} \tag{20}$$

This permits the identification of k in a physical model. The value of k in Fig.3 can be considered to represent the stiffness of a completely confined soil column of length L/4.

Substituting Eq.(20) in Eq.(11) gives the fundamental frequency of the system

$$\omega_1 = \frac{\pi v_s}{2h}\left[1 + \frac{64}{\pi^2}\frac{(1-\nu)}{(1-2\nu)}\left(\frac{h}{L}\right)^2\right]^{1/2} \qquad (21)$$

where $v_s = (G/\rho)^{\frac{1}{2}}$ is the velocity of shear waves in the soil. When Eq.(20) is employed in Eq.(17) the maximum pressure on the wall, p_o, is found to be

$$p_o = \frac{32 G S_{v1} (1-\nu)}{\pi \omega_1 L (1-2\nu)} \qquad (22)$$

For a typical value of Poisson's ratio ν, the ratio $(1 - \nu)/(1 - 2\nu)$ has the value 2. For initial design calculations, Eqs.(21), (22), (18) and (19) give the necessary maximum pressure, force and moment when the soil properties, wall proportions, and design earthquake are inserted. The effect of variations in some of the values can easily be ascertained.

(b) Properties increasing with depth.

In many soils, the elastic constants increase with depth, although the density can be considered to remain almost constant. To represent such cases, a solution is required to the problem of Fig.3 with G and k both functions of depth.

Solutions have been obtained for the cases where G is considered to be a general power function of depth, with ρ and k kept constant, and for the situation where density is constant, but k and G increase linearly with depth from zero or arbitrary values at the surface. These solutions are lengthy and will be presented elsewhere. In general they give rise to maximum first mode moments acting on the wall as a result of the maximum force being applied at a height of 0.6 to 0.7 of the wall height above the base.

However, one particular case of a variation of shearing modulus with depth has a special significance, as shown by Bielak (1), and will be analysed further. For this example, it is convenient to locate the zero x-cordinate at the base of the wall rather than at the top, and take x positive upwards. It will be assumed now that G(x) is parabolic with the equation

$$G = a(h^2 - x^2) \qquad (23)$$

where a is a constant. Here G is zero at ground surface and increases with depth.

The equation of motion is found to be

$$\frac{\partial^2 u}{\partial t^2} = \frac{a(h^2-x^2)}{\rho}\frac{\partial^2 u}{\partial x^2} - \frac{2ax}{\rho}\frac{\partial u}{\partial x} - \frac{2ku}{\rho b} \qquad (24)$$

On separating the variables, the motion is again found to be sinusoidal with time, and the equation governing the deflected shape of the shear beam, X(x) is

$$(h^2-x^2)\frac{\partial^2 X}{\partial x^2} - 2x\frac{\partial X}{\partial x} + \left(\frac{\rho\omega^2}{a} - \frac{2k}{ab}\right)X \qquad (25)$$

It is convenient to substitute the new variable s = x/h in Eq.(25) so that it becomes

$$(1-s^2)\frac{\partial^2 X}{\partial s^2} - 2s\frac{\partial X}{\partial s} + \left(\frac{\rho\omega^2}{a} - \frac{2k}{ab}\right)X \qquad (26)$$

This is the Legendre equation, whose solution is expressed in Legendre functions $P_p(s)$ of order p, where p is given by the equation

$$p(p+1) = \left(\frac{\rho\omega_n^2}{a} - \frac{2k}{ab}\right) \qquad (27)$$

The deflected shape of the beam is therefore given by the solution of Eq.(26), taking into account the boundary conditions

$$X = DP_p(s) \qquad (28)$$

The only Legendre functions which are finite at s = 1 (the top of the wall) are those in which p is an integer; these are the Legendre polynomials. However, X must be zero at s = 0, so that $P_p(0)$ must be zero, since D is non-zero. The Legendre polynomials which have zero value at s = 0 are those for which p is an odd integer. Consequently, the modes of vibration of the shear beam are found from Eq.(27) by substituting successively p = 1, 3, 5, etc.

The first mode has a particular interest in this special case. The Legendre polynomial $P_1(s)$ is a straight line, with equation

$$P_1(s) = s \qquad (29)$$

so that the shear beam remains straight as it oscillates in the first mode. All of the equations reduce to particularly simple forms in this circumstance. The first participation factor is 1.5, and the first natural frequency is

$$\omega_1 = \left[\frac{2a}{\rho} + \frac{2k}{b\rho}\right]^{1/2} \qquad (30)$$

The maximum pressure distribution on the wall is triangular, with the maximum at the top, and is given by the equation

$$p_{m_1} = p_o s \qquad (31)$$

where

$$p_o = \frac{1.5kS_{v1}}{\omega_1} \qquad (32)$$

The maximum force acting on the wall P_{m_1} is obtained from the area under the pressure diagram, as given by Eq.(31).

$$P_{m_1} = \tfrac{1}{2} p_o h \qquad (33)$$

Since the pressure distribution is triangular, the maximum force acts at a height of 2/3h from the base of the wall, so that the maximum moment M_{m_1} is found to be

$$M_{m_1} = \frac{1}{3} p_o h^2 \qquad (34)$$

Bielak (1) has demonstrated a further interesting and important property of this special case. Because of the linear nature of the first mode shape, and the orthogonality of the modes, no mode other than the first develops any base moment. Consequently, for a specified earthquake, the moment at the base of a rigid wall is given by Eq.(34) only; there are no additional moments due to the higher modes. The higher modes do, however, cause additional pressures and forces on the wall. The simple polynomial nature of the Legendre functions in this problem makes the contributions of the higher modes easy to calculate.

Linear first mode shapes also occur as special cases when variations of both G and k with depth are employed in the analysis. These will be discussed elsewhere.

(c) Boundary effects

For the constant property shear beam, the variation of the first mode frequency as the boundary AD in Fig.3 (or the other wall) becomes more distant from BC can be seen from Eq.(21). For values of L/h less than unity, it may be concluded intuitively that the model presented in this paper is not applicable; the two-dimensional nature of the real motion is important. The shear beam method probably represents the actual motion of the soil in a first mode realistically in the region L/h > 1.0. However, for L/h > 2 a second mode of vibration still describable by a shear beam can be recognised. In this mode, the vertical plane, half-way between AD and BC in Fig.3 becomes a node, and the soil in the contained space would be represented by two shear beams vibrating symmetrically. However this mode would not be excited by the rigid boundary conditions assumed here. The next mode to be excited under these restraints would be the antisymmetrical one with two nodal planes at the third points along the length L. When AD moves still further from BC the effect of the restraint conditions at AD become unimportant, and the pressures on the wall at BC become those of a wall restraining a backfill of unlimited extent. For this case, it is suggested that the calculational method described above still be employed, but with a value of L/h = 10. Thus the second term in the brackets of Eq.(21) will generally become negligible, but the value of k to be used in the pressure calculations, still based on L/4, will be 2.5h in these conditions.

(d) Effect of flexibility of wall

In reality a wall deflects both by bending and by rotation and translation on its base. The incorporation of bending deflections in the present analysis is complicated,

and a simpler treatment was adopted. A rigid wall hinged at its base was assumed. Only base rotations are represented, with rotational stiffness being accounted for by a torsional spring. Simplified calculations indicating the effect of wall flexibility are possible with this model if it is employed with the soil model associated with the Legendre equation, Eq.(26) which gives a linear first mode of vibration. For simplicity, the mass of the wall is neglected. In practice a mass of soil would accompany the wall in its vibrations, which could be significantly affected in consequence. In particular, phase differences between wall and soil vibrations would be possible. The simplified analysis is briefly described.

With a torque spring of value T at the base of the wall the equation of the angular deflection of the wall, θ, under moment M is

$$M = T\theta \tag{35}$$

Because the wall is rigid, the lateral displacement is linear with height. For a linear first mode, the dynamic lateral displacements of the soil shear beam are also linear with height, so that the pressure on the wall at any instant is given by k times the difference of the soil and wall displacements. The pressure thus also increases linearly with height as in the case of the rigid wall. The effect of the base rotation of the wall can thus be seen to be a reduction in the effective soil stiffness k. By consideration of the moment acting on the base of the wall it can be shown that the wall rotation gives rise to a new soil stiffness k' where

$$k' = \frac{1}{1 + \frac{kh^3}{3T}}\, k \tag{36}$$

Thus, for the first mode, Eqs.(30) and (32) still hold, but in them k must be replaced by k' from Eq.(36). Consequently, the pressures, forces and moments can be calculated as before but taking into account the wall rotation. By substituting appropriate values of various soil properties and reinforced concrete wall dimensions, it appears that in practice the factor modifying k in Eq.(36) will be around 0.5.

DISCUSSION

A solution to the problem of Fig.1 with linearly elastic soil, rigid wall, and a sine wave input was obtained by Matsuo and Ohara (3) under certain displacement restrictions. The forces and moments in the solutions presented here for a rigid wall are of the same magnitude as those shown by Matsuo and Ohara, and are significantly higher than those calculated by the Mononobe-Okabe method.[III] For the same problem and displacement restrictions, but with a hinged wall as in section (d) above, but including the wall mass, Ishii et al (2) gave a solution which they evaluated to show the phase domains.

Study of the appearance of real retaining walls following earthquakes as well as the model experiments gives rise to

[III] My interpretation of the results of Matsuo and Ohara (their Fig.17) is different from that of Seed and Whitman (their Figs.25 through 27).

the following hypothesis as to the sequence of events. Dynamic pressures and moments (higher than Mononobe-Okabe) act to cause wall movements during an earthquake. Irreversible soil displacements occur as the wall deflects away from the retained soil so that residual pressures develop and the wall deflections drift. Eventually partial or complete wall failure occurs with such a large deflection that a wedge of soil slides down behind the wall. On post-earthquake inspection the soil wedge is apparent and looks like confirmation of a Mononobe-Okabe failure mechanism. However, as indicated, the wedge formation is a post-failure condition. Partial failures of flood control channel walls in the 1971 San Fernando, California earthquake, and of the Showa bridge wing walls in the 1964 Niigata earthquake illustrate intermediate stages in the above sequence. Model experiments probably do not adequately represent full-scale wall behaviour during earthquakes.

ACKNOWLEDGMENT

This work was carried out with the assistance of U.S.A. National Science Foundation Grant No.G1-29937. Discussions with J.H.Wood, graduate student at the California Institute of Technology were of great assistance.

REFERENCES

(1) BIELAK, J., Proc.Amer.Soc.Civ.Eng., 95, Jour.Eng.Mech.Div., EM5, Oct.1969.
(2) ISHII, Y., ARAI, M., and H.TSUCHIDA, Proc.2nd World Conf. Earthqu.Eng., 1, 211-230, 1960.
(3) MATSUO, M., and S.OHARA, Proc.2nd World Conf.Earthqu. Eng. 1, 165-173, 1960.
(4) MONONOBE, N., Proc.World Engineering Congress, 9, 275, 1929.
(5) OKABE, S., Jour.Japanese Soc.Civ.Eng., 12, No.1, 1926.
(6) SEED, H.B. and R.V.WHITMAN, Conference on Lateral Stresses and Earth-Retaining Structures, Amer.Soc. Civ.Eng., 103-147, 1970.
(7) WOOD, J.H., Personal communication, 1971.

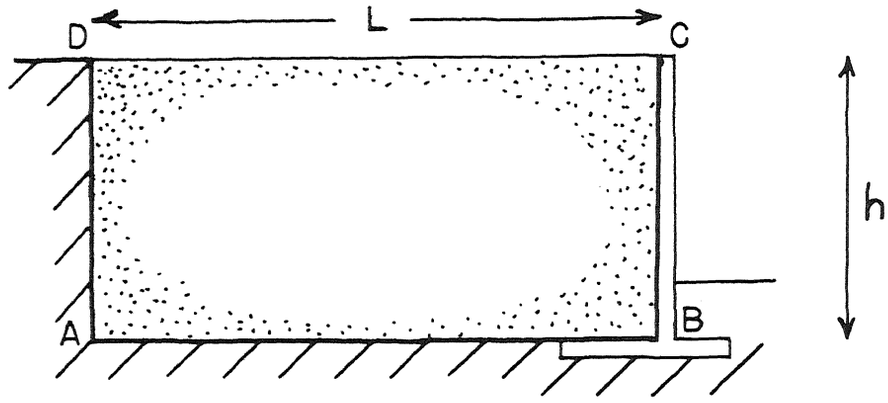

FIG.1 REGION OF PROBLEM

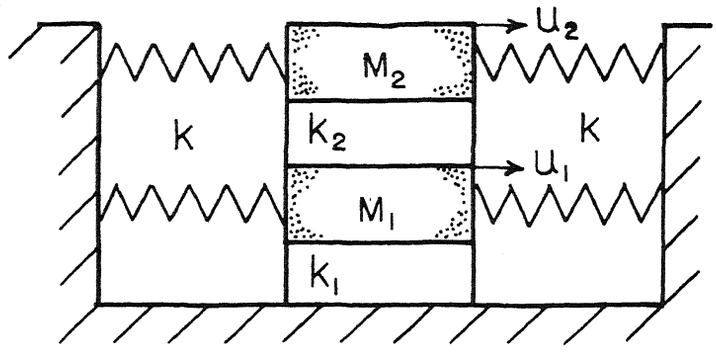

FIG.2 LUMPED PARAMETERS

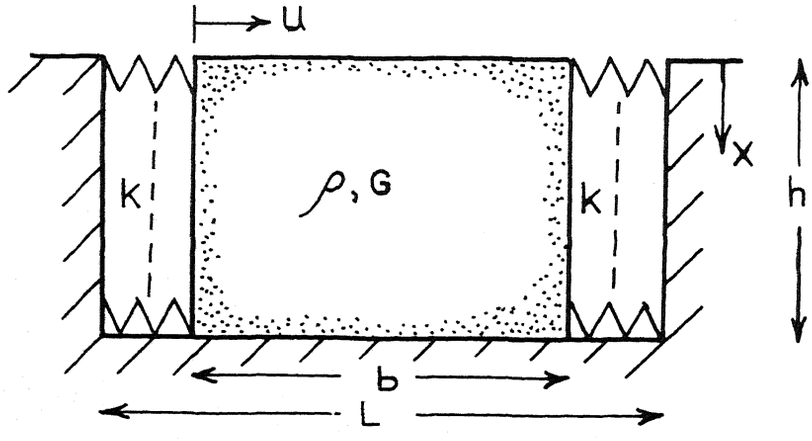

FIG.3 CONTINUOUS SHEAR BEAM